Available online at www.sciencedirect.com
ScienceDirect
Journal of Nuclear Materials 367–370 (2007) 834–838
journal of nuclear materials
www.elsevier.com/locate/jnucmat

Creep mechanism of highly purified V–4Cr–4Ti alloys during thermal creep in a vacuum

Ken-ichi Fukumoto [a,*], Takuya Nagasaka [b], Takeo Muroga [b], Nobuyasu Nita [c], Hideki Matsui [c]

[a] *Graduate School of Nuclear Power and Energy Safety Engineering, University of Fukui, Bunkyo 2-1-1, Fukui 910-8507, Japan*
[b] *National Institute for Fusion Science, Toki, Gifu 509-5292, Japan*
[c] *Institute for Materials Research, Tohoku University, Sendai 980-8577, Japan*

Abstract

Pressurized thermal creep tubes of highly purified V–4Cr–4Ti, the NIFS-Heat-2 alloy have been examined following testing in the range 700–850 °C. It was found that the creep stress exponent of the NIFS-Heat-2 alloy is about five and that the characteristic creep mechanism was the dislocation creep usually observed in pure metals. The apparent activation energy of creep deformation is about 210 kJ/mol in the temperature range 700–850 °C. Creep deformation was considered to be controlled by climb-controlled dislocation-glide at 850 °C, where sub-grain boundary structure predominates and consists of dislocation dipole structures and pile-ups of dislocations.

1. Introduction

Vanadium alloys are candidate materials for fusion reactor blanket structural applications because of their potentially high operation temperatures. However, the knowledge about the creep properties of vanadium alloys at fusion-relevant temperatures is limited and there are uncertainties that may have influenced the results such as the interstitial impurity content of specimens. In order to measure irradiation creep, several tests have been done using pressurized creep tubes (PCTs) [1–3]. Recently, high-purity V–4Cr–4Ti ingots (NIFS-Heat-1 and 2) were provided by the National Institute for Fusion Science (NIFS), Japan [4–6]. In order to perform creep tests on highly purified V–4Cr–4Ti alloys, a manufacturing process for pressurized creep tubes has been established with the aim of avoiding contamination by interstitial impurities during the process [6,7].

The objective of this study is to investigate the thermal creep properties and microstructural changes of a highly purified V–4Cr–4Ti alloy, the NIFS-Heat-2, by using PCTs, as a preliminary study to enable future in-pile creep tests.

2. Experimental Procedures

The V–4Cr–4Ti alloy used in this study was produced by NIFS and Taiyo Koko Co. and is designated NIFS-Heat-2 [5]. The detailed fabrication

* Corresponding author. Tel./fax: +81 776 27 9712.
E-mail address: fukumoto@mech.fukui-u.ac.jp (K.-i. Fukumoto).

0022-3115/$ - see front matter © 2007 Elsevier B.V. All rights reserved.
doi:10.1016/j.jnucmat.2007.03.074

Table 1
Creep test conditions for NIFS-Heat-2 PCTs

Test temperature (°C)	700	750	800	850
Tubing annealed 2 h at 1000 °C				
Effective stress (MPa)	200	200	200	
	150	150	150	150[a]
	110	100	90	100[a]
			70	
			50	
As-drawn tubing				
Effective stress (MPa)				137

[a] Indicates that TEM observations have been performed on that specimen.

processes for tubing and for PCTs have been reported [6,7]. Table 1 shows the creep test conditions for PCTs. The PCTs wrapped with Ta and Zr foils were encapsulated in a quartz tube in a vacuum of $<\sim 5\times10^{-3}$ Pa. In order to remove gas impurities from the quartz tube, about 100 cm^2 of Zr foil were included as a getter. Thermal creep tests were performed by placing the sealed quartz tubes in a muffle furnace. Dimensional changes of PCTs were measured with a precision laser profilometer manufactured by KEYENCE, LM-7030MT. Diameters were determined to an accuracy of ±1 μm. When the creep strain exceeded 20%, the creep test was terminated. Transmission electron microscopy (TEM) observations were performed on pieces cut from selected PCTs. The detailed fabrication procedure for TEM specimens from PCTs has been reported [2]. TEM observations were performed using a JEOL-2000FX at the University of Fukui. Chemical analyses for oxygen and nitrogen were performed on two of the 850 °C PCT specimens using the rest of the specimens.

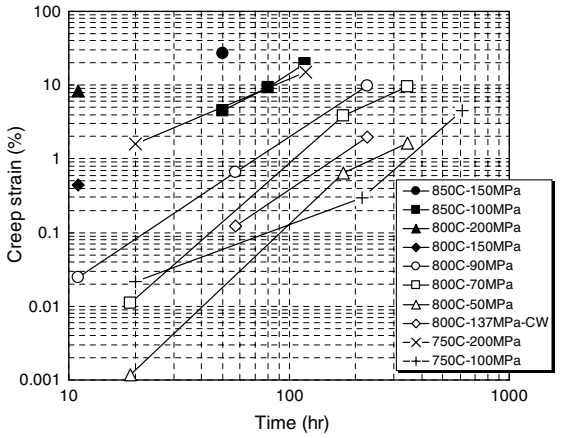

Fig. 1. Time dependence of the effective mid-wall creep strain of a highly purified V–4Cr–4Ti, the NIFS-Heat-2 alloy for the 700, 750, 800 and 850 °C test temperatures.

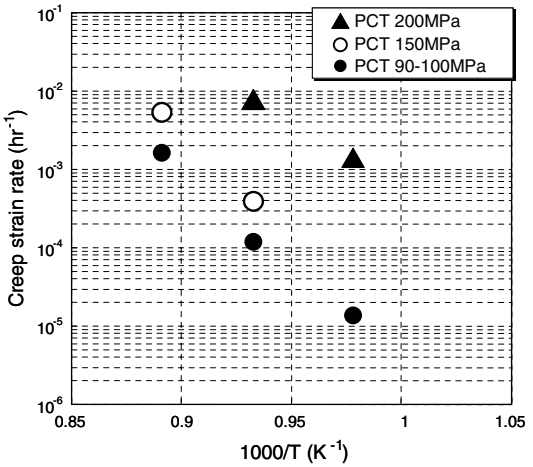

Fig. 2. Arrhenius plot of creep strain rate of a highly purified V–4Cr–4Ti, the NIFS-Heat-2 alloy. Stress levels are 200, 150 and 90–110 MPa.

3. Results

3.1. Creep strain measurement

Fig. 1 shows the time dependence of the effective mid-wall creep strain for 700 °C, 750 °C, 800 °C and 850 °C test temperatures. In Fig. 1, primary creep cannot be observed as the duration of primary creep is expected to be short [8,9].

Fig. 2 shows an Arrhenius plot of creep strain rate obtained from data in Fig. 1. Creep strain rates were determined by using data for effective strains less than about 1% to exclude any ternary creep data, even though the remaining number of data are few. From Fig. 2, the activation energy for creep of V–4Cr–4Ti was estimated for effective stress levels of approximately 100 and 150 MPa. Activation energies ranging from 197 to 227 kJ/mol were obtained, with an average value of 210 kJ/mol. The activation energies do not vary inversely with stress as has been observed for pure vanadium [8,10]. These values are similar to those obtained for the NIFS-Heat in uniaxial creep tests about 180–210 kJ/mol in the 750–800 °C temperature range [9]. However, these values are somewhat smaller than the activation energy for self diffusion in pure vanadium, which is about 270 kJ/mol in the 700–800 °C temperature range [8,11].

The stress dependence of creep strain rate was also deduced from Fig. 1. The data in Fig. 1 were fitted with the equation $d\varepsilon/dt = A\sigma^n$, where A is a constant, n the creep stress exponent, ε the effective creep strain rate and σ is the effective stress. The stress exponent was found to be 4.9 for 800 °C creep data. It has been reported that the strain exponents, n, for pure V and V–Ti alloys [10,12,13] are greater than 5 for creep test conditions similar to those used in this work, indicating that the creep mechanism is climb-assisted glide of dislocations.

The average oxygen and nitrogen levels have been measured to be 330 and 110 wppm after 51 h, and 520 and 140 wppm after 118 h for the 850 °C PCT specimens. On the other hand, the oxygen content and the nitrogen content were 270 wppm and 110 wppm after 660 h for the 750 °C PCT specimens, respectively. These levels may be compared to the as-received values of 370 wppm O and 100 wppm N. It is indicated that impurity pick up does not occur in creep tests with a quartz tube due to careful sealing treatment. However, there is a possibility that residual gas impurity unexpectedly remained in the quartz tube and was absorbed by some specimens during vacuum encapsulation.

4. Microstructural analysis

The two specimens tested at 850 °C were selected for TEM observation and for chemical analyses in order to identify the operating creep mechanism. TEM micrographs of the NIFS-Heat-2 alloy tested at 850 °C are presented in Fig. 3. Moderately high dislocation densities can be seen in the 100 MPa specimen, where the dislocations tend to be confined to sub-grain boundaries like cell structures and to lie in randomly arrays inside the sub-grains. On the other hand, dislocation cell structures are fully developed in a uniform array at regular intervals of about 0.8 μm in the 150 MPa specimen. Precipitates of Ti(OCN) are located in non-uniform distributions in grains and/or at grain boundaries. The precipitate particles were present prior to testing and did not change significantly as a result of creep testing; they are similar in size to those reported by Heo et al. [14]. In order to identify the dislocation Burgers vectors, the $\boldsymbol{g}\cdot\boldsymbol{b}=0$ technique was applied. Such an analysis revealed that most of the free dislocations not associated with sub-grain boundaries in the 100 MPa specimen are of the $a/2\langle 1\,1\,1\rangle$ type. Fig. 4 shows TEM images of a dislocation array in the specimen tested at 850 °C at a stress of 150 MPa. The straight dislocations running from upper left to lower right consist of dislocations with two types of Burgers vector, $[1\,1\,1]$ and $[\bar{1}\,1\,1]$. Orientation trace analysis show they are edge dislocations. Therefore, this dislocation array consists of edge dipoles made of different types of dislocations. Other examples were found showing that the sub-grain boundaries were comprised mainly of edge dislocations.

5. Discussion

Both uniaxial [9,15] and biaxial [8,16] creep tests were performed in vacuum with different starting concentrations of interstitial O in recent studies. A review of thermal creep of V–Cr–Ti alloys by Kurtz et al. [16], found the activation energy for creep between 700 and 800 °C to be about 300 kJ/mol, which is similar to the activation energy for self-diffusion in pure V. This suggests that in this regime of

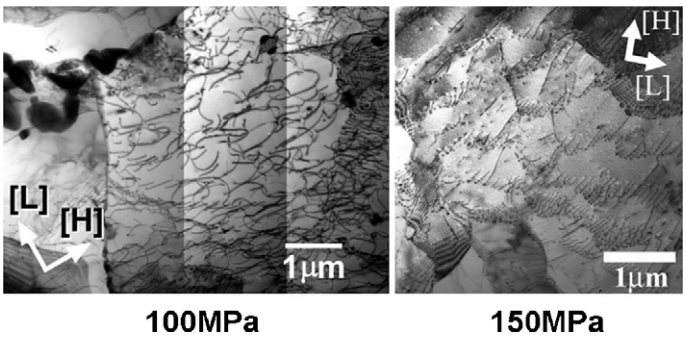

Fig. 3. Examples of TEM images of a highly purified V–4Cr–4Ti, the NIFS-Heat-2 alloy, tested at 850 °C under creep stresses of 100 MPa and 150 MPa. Arrows indicate the directions related to the pressurized creep tube geometry; [L] indicates a longitudinal direction along the tube and [H] a hoop direction.

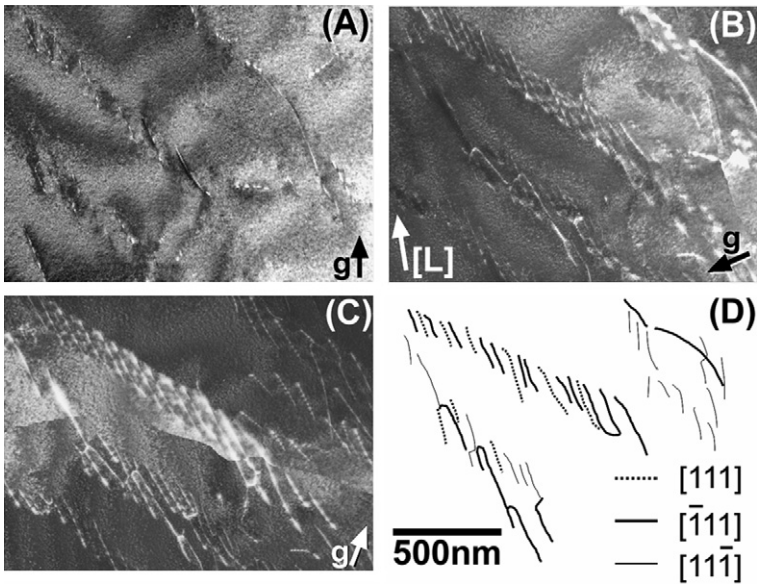

Fig. 4. Examples of TEM images of dislocation structures in the V–4Cr–4Ti alloy tested at 850 °C with a stress of 150 MPa. (A) $(1\bar{1}0)$ diffraction vector, (B) $(\bar{1}21)$ diffraction vector, (C) (121) diffraction vector, and (D) a characterization map for Burgers vector of dislocations. The arrow inserted in each photo shows the direction of the g-reflection.

temperature and stress the predominant creep mechanism is climb-assisted dislocation motion. The apparent activation energy in the present study is 210 kJ/mol for stresses between 100 and 150 MPa. These values are lower than the activation energy found for the US-Heat #832665 of V–4Cr–4Ti, 299 kJ/mol [8], and higher than the values found for V–2.8Ti, 125 kJ/mol [12,17]. It has been reported that the strong scavenging effect of titanium and low oxygen solubility in V–3Ti correspond to the lowest activation energy for creep in V–Ti alloys [11]. This result indicated that the oxygen content may be significantly lower in V–3Ti than in any other V–Ti alloy and that the reduction of matrix impurity contents may lead to a lower activation energy. The reduction in oxygen and interstitial impurity content, may explain why the activation energies for NIFS-Heat alloys are lower than the energy for other V–4Cr–4Ti alloys containing above 1000 wppm of O, C, N. It suggests that the reduction of impurity content lowers the potential barrier for vacancy diffusion and impurities in V–Cr–Ti alloys act as trapping site for vacancies, leading to the formation of Ti solute – impurity – vacancy complexes. It is also possible these complexes are obstacles to climb-assisted vacancy diffusion to dislocation cores in these creep conditions.

The power law dependence of the secondary creep rate on stress with $n = 4.9$, in this study is in good agreement with the value of stress exponent of $n = \sim 4$ reported in a review of thermal creep for V–4Cr–4Ti by Kurtz [16]. This result also suggests that the operating creep mechanism is climb-assisted dislocation motion and this idea is supported by the microstructural analysis. The cell structure formation occurring during thermal creep also indicates that the creep mechanism is of pure metal type and that dislocation core diffusion plays an important role as the rate controlling process for creep deformation. The cell structure is made of arrays of edge dislocation dipoles formed during thermal creep and did not result from post-creep deformation. The other dislocation arrays made of dislocations with one type of Burgers vector also appears to be formed during thermal creep. Both types of dislocation arrays formed in the same grain without free dislocations between cell walls indicating no post-creep deformation. The dependence of the microstructure on stress also suggests that at high stresses glide-controlled creep behavior predominates over the climb-controlled creep such that free dislocations in a sub-grain are absorbed in the sub-grain walls. The increase in density of free dislocations between sub-grain boundaries at lower stress levels indicates that climb-controlled creep dominates and dislocations then distribute randomly. With increasing density of free dislocations, the creep stress exponent gradually decreases to a

value of about three, indicating a solid-solute creep behavior [18]. Since the target of this study was to explore creep deformation under moderately high stress level, the data are not sufficient to establish the creep mechanism diagram for V–4Cr–4Ti. Further work at lower stresses and elevated temperatures are needed to determine the thermal creep mechanisms as a baseline for future irradiation creep measurements.

6. Summary

In order to investigate the thermal creep properties and microstructural changes of the highly purified NIFS-Heat-2 V–4Cr–4Ti, thermal creep tests were performed in the range 700–850 °C using PCTs. The creep stress exponent for the NIFS-Heat-2 alloy was about 5 which is characteristic of dislocation-glide creep observed in pure metals. The apparent creep activation energy of creep deformation was about 210 kJ/mol in the temperature range 750–800 °C. Microstructural analysis showed dislocation cell structures developed at 850 °C under the highest applied stress. This also suggests that climb-assisted glide of dislocations is the rate-limiting creep process at 850 °C.

Acknowledgement

This work was supported by NIFS Budget Code, NIFS04KFRF010.

References

[1] H. Tsai, H. Matsui, M.C. Billone, R.V. Strain, D.L. Smith, J. Nucl. Mater. 258–263 (1998) 1471.
[2] K. Fukumoto, S. Takahashi, R.J. Kurtz, D.L. Smith, H. Matsui, J. Nucl. Mater. 341 (2005) 83.
[3] J.M. Vitek, D.N. Braski, J.A. Horak, J. Nucl. Mater. 141–143 (1986) 982.
[4] T. Muroga, T. Nagasaka, A. Iiyoshi, A. Kawabata, S. Sakurai, M. Sakata, J. Nucl. Mater. 283–287 (2000) 711.
[5] T. Muroga, T. Nagasaka, K. Abe, V.M. Chernov, H. Matsui, D.L. Smith, Z.-Y. Xu, S.J. Zinkle, J. Nucl. Mater. 307–311 (2002) 547.
[6] T. Nagasaka, T. Muroga, T. Iikubo, Fusion Sci. Technol. 44 (2003) 465.
[7] K. Fukumoto, H. Matsui, M. Narui, T. Nagasaka, T. Muroga, J. Nucl. Mater. 335 (2004) 103.
[8] R.J. Kurtz, M.L. Hamilton, J. Nucl. Mater. 283–287 (2000) 628.
[9] K. Fukumoto, T. Yamamoto, S. Nakao, S. Takahashi, H. Matsui, J. Nucl. Mater. 307–311 (2002) 610.
[10] K.R. Wheeler, E.R. Gilbert, F.L. Yaggee, S.A. Duran, Acta Metall. 19 (1971) 21.
[11] D.L. Harrod, R.E. Gold, Int. Met. Rev. 4 (1980) 163.
[12] H. Boehm et al., J. Less-Common Met. 12 (1967) 280.
[13] T. Kainuma, N. Iwao, T. Suzuki, R. Watanabe, J. Less-Common Met. 86 (1982) 263.
[14] N.J. Heo, T. Nagasaka, T. Muroga, J. Nucl. Mater. 325 (2004) 53.
[15] K. Natesan, W.K. Soppet, A. Purohit, J. Nucl. Mater. 307–311 (2002) 585.
[16] R.J. Kurtz, K. Abe, V.M. Chernov, D.T. Hoelzer, H. Matsui, T. Muroga, G.R. Odette, J. Nucl. Mater. 329–333 (2004) 47.
[17] H. Boehm et al., Z. Metallkd. 59 (1968) 715.
[18] J. Cadek, Creep in Metallic Materials, Elsevier, 1988, p. 115.